Acta Crystallographica Section D
Biological Crystallography
ISSN 0907-4449

Crystallization and low-resolution structure of an effector-caspase/P35 complex: similarities and differences to an initiator-caspase/P35 complex

Michael J. Eddins,[a] Donna Lemongello,[a] Paul D. Friesen[b] and Andrew J. Fisher[a,c]*

[a]Department of Chemistry, University of California, Davis, CA 95616, USA, [b]Institute for Molecular Virology and Department of Biochemistry, University of Wisconsin, Madison, WI 53706, USA, and [c]Section of Molecular and Cellular Biology, University of California, Davis, CA 95616, USA

Correspondence e-mail: fisher@chem.ucdavis.edu

Received 7 September 2001
Accepted 5 November 2001

The aspartate-specific caspases play a pivotal role in the execution of programmed cell death and therefore constitute important targets for the control of apoptosis. Upon ectopic expression, baculovirus P35 inhibits apoptosis in phylogenetically diverse organisms by suppressing the proteolytic activity of the cellular caspases in a cleavage-dependent mechanism. After cleavage by caspase, the P35 fragments remain bound to the target caspase, forming an inhibitory complex that sequesters the caspase from further activity. Crystals of a complex between P35 and *Sf*-caspase-1, an insect effector-caspase, were grown. A 5.2 Å resolution structure of this inhibitory complex was determined by molecular-replacement methods. The structure reveals few regions of interaction between the two proteins, much like that observed in the structure of the recently solved human initiator-caspase/P35 complex. In the effector-caspase/P35 complex structure presented here, the P35 molecule shifts towards a loop that is conserved in effector caspases but absent in initiator caspase. This shift could strengthen interactions between the two proteins and may explain the preference of P35 for inhibiting effector-caspases.

1. Introduction

Apoptosis, or programmed cell death, is a multistep process leading to the destruction of the cell. The regulation of apoptosis is essential for the viability of metazoans (Ashkenazi & Dixit, 1998). This process is vital for normal development, tissue homeostasis and defense against viral pathogenesis (Thompson, 1995).

Diverse signals initiate apoptosis and culminate in the activation of a highly conserved pathway utilizing a group of aspartate-specific cysteinyl enzymes called caspases (Nicholson & Thornberry, 1997). These proteases exist in the cell as dormant proenzymes. Upon proteolytic activation by initiator caspases, the effector caspases cleave vital cellular components, leading to the death of the cell (Casciola-Rosen *et al.*, 1996; Ahmad *et al.*, 1997; Thornberry & Lazebnik, 1998). The activation and activity of the caspases are decisive control points in the apoptotic process making them attractive for intervention (White, 1996).

Upon viral infection, cells activate their apoptotic pathway, sacrificing themselves to prevent virus propagation (Hardwick, 1997). To counteract these measures in order to replicate, viruses have evolved diverse anti-apoptotic genes that regulate this process (Shen & Shenk, 1995). The baculovirus gene *p35* blocks virus-induced apoptosis in host insect cells. Moreover, it is a general apoptotic suppressor in phylogenetically diverse organisms when expressed ectopically (Cartier *et al.*, 1994; Sugimoto *et al.*, 1994; Beidler *et al.*, 1995). Protein P35 blocks apoptosis by acting as a substrate inhibitor for the active form of the caspases. Caspase inhibition requires P35 cleavage and a subsequent conformational change to form a stable complex with the caspase (Bump *et al.*, 1995; Bertin *et al.*, 1996; Fisher *et al.*, 1999).

To understand the mechanism of viral P35 inhibition of the caspases, we have crystallized and determined the low-resolution three-dimensional structure of P35 bound to an active effector-caspase. Crystals have been grown of P35 complexed with the insect effector-caspase *Sf*-caspase-1, which is likely to be the natural target that P35 evolved to inhibit in infected *Spodoptera frugiperda* larvae (Ahmad *et al.*, 1997). These crystals currently diffract to 5.2 Å resolution, which allowed the low-resolution structure to be determined by molecular-replacement methods. The structure shows the relative orientation of P35 with respect to the inhibited caspase and the surfaces of contact. To determine how P35 interacts with different classes of caspases, this

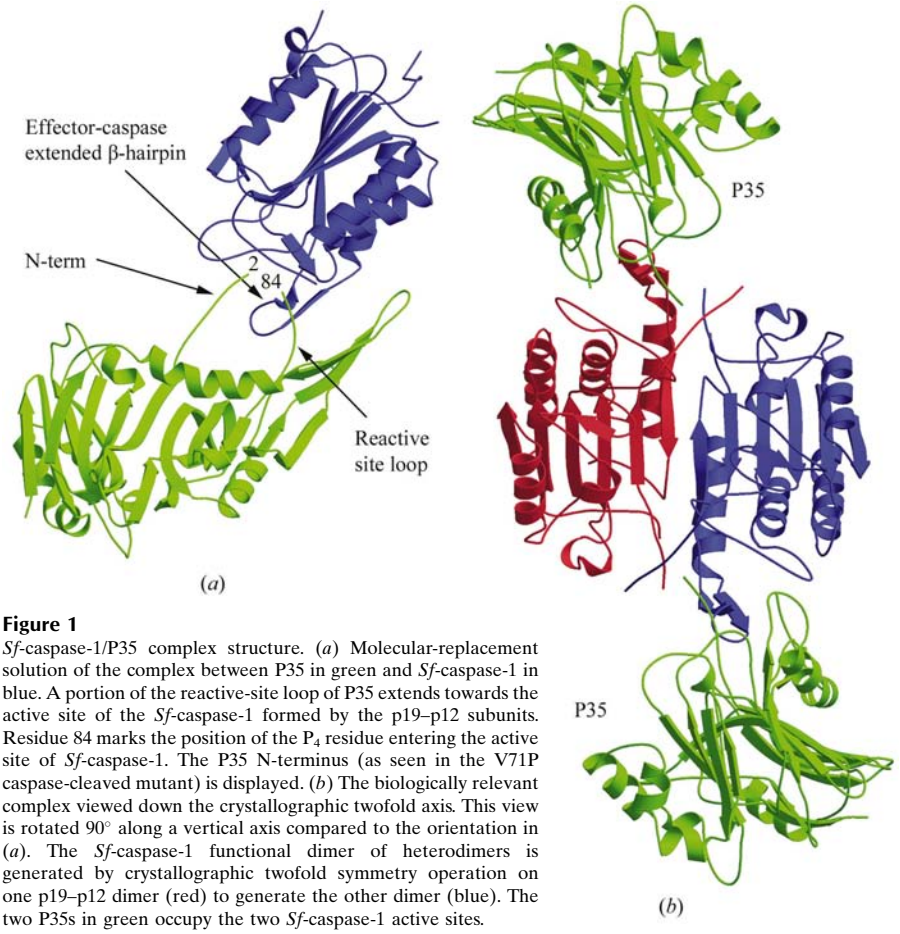

Figure 1
Sf-caspase-1/P35 complex structure. (*a*) Molecular-replacement solution of the complex between P35 in green and *Sf*-caspase-1 in blue. A portion of the reactive-site loop of P35 extends towards the active site of the *Sf*-caspase-1 formed by the p19–p12 subunits. Residue 84 marks the position of the P_4 residue entering the active site of *Sf*-caspase-1. The P35 N-terminus (as seen in the V71P caspase-cleaved mutant) is displayed. (*b*) The biologically relevant complex viewed down the crystallographic twofold axis. This view is rotated 90° along a vertical axis compared to the orientation in (*a*). The *Sf*-caspase-1 functional dimer of heterodimers is generated by crystallographic twofold symmetry operation on one p19–p12 dimer (red) to generate the other dimer (blue). The two P35s in green occupy the two *Sf*-caspase-1 active sites.

structure is compared with that of a recently solved initiator-caspase/P35 complex (Xu *et al.*, 2001).

2. Methods

2.1. Preparation, crystallization and data collection

Recombinant P35 was expressed in *Escherichia coli* as described previously (Fisher *et al.*, 1999). *Sf*-caspase-1 from *S. frugiperda* plus a C-terminal His-tag extension was also expressed in *E. coli* as described by Manji & Friesen (2001). Bacterial pellets were resuspended in reaction buffer (20 m*M* PIPES pH 7.4, 100 m*M* NaCl, 1 m*M* EDTA, 5 m *M* DTT, 10% sucrose, 0.1% CHAPS) and mixed and lysed to generate a molar excess of P35. The soluble cell lysate was incubated for 12 h at room temperature, after which the lysate was dialyzed against 500 m*M* NaCl, 50 m*M* $NaHPO_4$, 0.5 m*M* imidazole pH 8.0 and purified over two metal-chelate columns and a cation-exchange column.

The *Sf*-caspase-1-His_6/P35 complex was crystallized by hanging-drop vapor diffusion using 2 µl drops of the complex (15 mg ml^{-1}) mixed with an equal volume of reservoir buffer [100 m*M* cacodylate pH 6.5, 12%(*w*/*v*) PEG 8000, 100 m*M* NaCl, 150 m*M* magnesium formate, 20% glycerol]. Crystals of approximate dimensions 0.4 × 0.1 × 0.1 mm grew within one week at room temperature and four weeks at 277 K and belong to the tetragonal space group $P4_32_12$, with unit-cell parameters $a = b = 76.9$, $c = 378.3$ Å. The enantiomorphic space group $P4_12_12$ was ruled out by molecular-replacement solution (see below). The Matthews coefficient V_M was calculated to be 4.18 Å^3 Da^{-1} (~70.3% solvent) assuming one p19–p12 *Sf*-caspase-1 dimer and a P35 monomer per asymmetric unit (ASU) (Matthews, 1968). Crystals were frozen in the mother liquor to 103 K for data collection. X-ray diffraction data were collected on beamline 7-1 at SSRL ($\lambda = 1.08$ Å) to a resolution of 5.2 Å. Oscillation data were collected with a MAR image-plate detector positioned at a crystal-to-detector distance of 450 mm. Crystals were exposed for 10 min with an oscillation angle of 2.0°. Diffraction data were processed with *DENZO* and scaled with *SCALEPACK* (Otwinowski & Minor, 1997). Data statistics are given in Table 1.

Table 1
Data-collection and processing statistics.

Space group	$P4_32_12$
X-ray source	SSRL beamline 7-1
Wavelength (Å)	1.08
Unit-cell parameters (Å)	$a = b = 76.9$, $c = 378.3$
Matthews coefficient (Å^3 Da^{-1})	4.18
Estimated solvent content (%)	70.3
Diffraction limit (Å)	5.2
No. of observations	24002
No. of unique reflections	5595
Completeness (%)	94.7
$R_{\rm merge}$† (%)	9.6

† $R_{\rm merge} = (\sum_h \sum_i I_h - I_{hi}|/\sum_h \sum_i I_{hi}) \times 100$, where I_h is the mean of the I_{hi} observations of reflection h.

A model for *Sf*-caspase-1 was determined by *SWISS-MODEL* (Appel *et al.*, 1994) from the Swiss Institute of Bioinformatics (SIB) using human-caspase-3 as a template (40% sequence identity; 60% sequence homology). This produced an *Sf*-caspase-1 model that was similar to the human-caspase-3 structure (1.1 Å r.m.s.d).

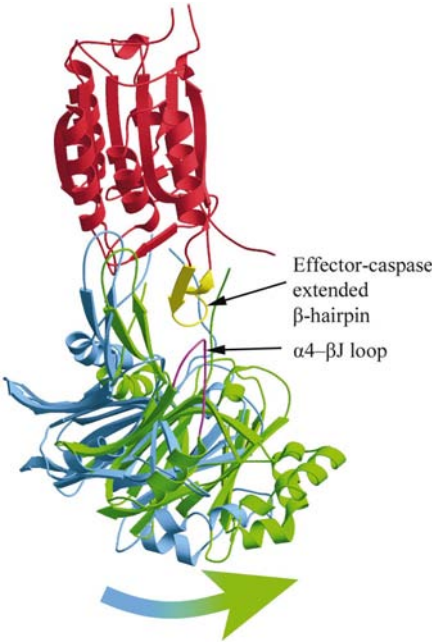

Figure 2
Overlay of the two P35 structures as observed in two caspase/P35 complex structures. The initiator-caspase/P35 and effector-caspase/P35 complexes were structurally aligned based on superposition of the caspase subunits, of which only the *Sf*-caspase-1 structure is shown in red. Shown in blue is the placement of P35 as observed in the initiator-caspase/P35 crystal structure. The effector-caspase/P35 complex structure reveals a rotation of P35 (green) towards an extended β-hairpin loop (yellow) that is structurally conserved in effector caspases only. This could generate additional interactions between this caspase loop and the $\alpha4$–βJ loop of P35 (purple).

The evolutionary-search molecular-replacement algorithm in the program *EPMR* (Kissinger *et al.*, 1999) was used to solve the structure. Six initial independent searches were calculated in both enantiomorphic space groups $P4_32_12$ and $P4_12_12$ using three different models: P35 wild type (Fisher *et al.*, 1999), cleaved V71P mutated P35 (delaCruz *et al.*, 2001) and the *Sf*-caspase-1 model (based on the human caspase-3 structure). The V71P caspase-cleaved P35 mutant in space group $P4_32_12$ resulted in the strongest peak, with a correlation coefficient and an *R* factor of 0.53 and 59%, respectively (false solutions had correlation coefficients and *R* factors of ~0.41 and 65%, respectively). After fixing the P35 mutant structure, the *Sf*-caspase-1 model was used in a subsequent search in space group $P4_32_12$. The final solution after rigid-body refinement yielded a correlation coefficient of 0.618 and an *R* factor of 54.7% to 5.2 Å resolution. All the false solutions in the second search had correlation coefficients and *R* factors of around 0.50 and 60%, respectively.

3. Results and discussion

The solution from molecular replacement placed the caspase recognition and cleavage site of P35 (DQMD[87]) into the active-site cleft of the caspase (Fig. 1*a*). The *Sf*-caspase-1/P35 complex solution is situated at a crystallographic twofold symmetry axis, generating the biologically relevant complex of a *Sf*-caspase-1 dimer of dimers consisting of two p19 subunits and two p12 subunits, and two P35 monomers (Fig. 1*b*). Outside the active-site region, the other main regions of interactions between the caspase and P35 are limited to the βK–βL hairpin loop from P35, which approaches a structurally conserved helix of *Sf*-caspase-1 (Fig. 1*a*). Additionally, an extended β-hairpin loop region from the *Sf*-caspase-1 model (residues 265–277) approaches and could potentially interact with residues P_5–P_3 of the reactive-site loop and the α4–βJ loop of P35 (Fig. 1*a*). The crystal structure of V71P-mutated P35 after caspase cleavage revealed that the N-terminus is released from the main body of the protein and assumes an extended conformation (delaCruz *et al.*, 2001). At the resolution of the complex reported here, individual peptide chains cannot be deciphered, yet the position of the P35 N-terminus as seen in caspase-cleaved V71P-mutated P35 modeled into the context of the complex places the N-terminus of P35 near the caspase active site.

A structure of an initiator human caspase-8/P35 complex at 3.0 Å shows similar interactions between the initiator caspase-8 and P35, but in higher detail (Xu *et al.*, 2001). This structure revealed that a covalent thioester bond forms between the active-site cysteine of the caspase and the carbonyl of the P_1 Asp87 in the caspase recognition site of P35. Additionally, the N-terminus of P35 extends out and interacts with the active-site histidine residue of caspase-8, preventing activation of a water molecule. Thus, P35 traps the enzyme at the thioester intermediate state of proteolysis (Xu *et al.*, 2001). Furthermore, the βK–βL loop of P35 interacts with a structurally conserved loop and helix of caspase-8.

Comparison of the structures of the two complexes reveals some differences that can be observed at 5.2 Å resolution. The main difference between the initiator-caspase/P35 complex and the effector-caspase/P35 complex is the relative orientation or angle between P35 and the caspase (Fig. 2). This suggests there is some conformational flexibility between the two proteins. This flexibility may allow P35 to inhibit a wider variety of caspases by accommodating the different structural surfaces from the distinct caspases.

Many of the interactions in the effector-caspase/P35 complex are similar to those observed in the initiator-caspase/P35 complex. The formation of the covalent thioester to the active-site cysteine is presumed to be the same, but at the resolution reported here (5.2 Å) it is impossible to be certain. The main difference is the interactions outside the caspase active site arising from the different global disposition of P35 with respect to caspase (Fig. 2). The rotation of P35 generates new possible interactions that are unique to the effector caspases. P35 swivels towards an extended β-hairpin loop region of the effector-caspase, which is likely to mediate new interactions with residues P_5–P_3 of the reactive-site loop and the α4–βJ loop of P35 (Fig. 2). This extended β-hairpin loop from the insect caspase model is only found in the effector-caspases and is absent from the initiator-caspases (based on structural and sequence data; Rotonda *et al.*, 1996; Cohen, 1997). The flexibility of its reactive-site loop may help P35 inhibit most of the caspases *in vitro*, but *in vivo* the extra residues in the extended loop of the effector-caspases may make it a more favorable binding partner to P35.

It has recently been shown that P35 does not inhibit certain initiator-caspases *in vivo* (Vier *et al.*, 2000; Manji & Friesen, 2001). Human caspase-9 is an example of an initiator-caspase that is not inhibited by P35 in cell-free extracts (Vier *et al.*, 2000). Additionally, another initiator-caspase (*Sf*-caspase-X) from *S. frugiperda* is resistant to P35 inhibition *in vivo* (Manji & Friesen, 2001) and the *Drosophila* caspase DRONC is also unyielding to P35 inhibition (Hawkins *et al.*, 2000).

The *Sf*-caspase-1/P35 complex is the physiologically relevant complex (Ahmad *et al.*, 1997). Human initiator-caspase-8 is not a natural target of P35. Moreover, the caspase recognition site of P35 seems to be tailored to inhibit the effector-caspases because of the presence of Asp in the P_4 position, which is preferred for effector caspases (Zhou *et al.*, 1998). Neither of these P35/caspase complex structures explains exactly why P35 inhibits both initiator- and effector-caspases *in vitro*. One possibility is that since the initiator-caspases prefer Ile/Leu/Val in the P_4 position and do not strictly require it, they may have some tolerance for aspartate found in P35. The aspartate is not a large side chain and the caspase-8/P35 complex structure reveals that it fits in the initiator-caspase active-site cleft (Xu *et al.*, 2001). In the *in vitro* caspase-inhibition studies, the protein concentrations are high with no competing proteins (Zhou *et al.*, 1998), which may help force the formation of the initiator-caspase/P35 inhibitory complex that might not occur or be stabilized *in vivo*. Within the apoptotic cell, the extended loop conserved in the effector-caspases may contribute to stronger interactions with P35 in combination with the aspartate in the P_4 position.

It remains to be seen if P35 is unable to inhibit other initiator-caspases *in vivo* like human caspase-8 or if the P35-resistant initiator caspases are limited to a subset that interacts with Apaf-1 or CED-4 such as caspase-9 or possibly the *Sf*-caspase-X and DRONC. Methods are earnestly being pursued to improve diffraction quality of these effector-caspase/P35 complex crystals in order to determine the structural basis for the preference of P35 for effector caspases.

References

Ahmad, M., Srinivasula, S. M., Wang, L., Litwack, G., Fernandes-Alnemri, T. & Alnemri, E. S. (1997). *J. Biol. Chem.* **272**, 1421–1424.

Appel, R. D., Bairoch, A. & Hochstrasser, D. F. (1994). *Trends Biol. Sci.* **19**, 258–260.

Ashkenazi, A. & Dixit, V. M. (1998). *Science*, **281**, 1305–1308.

Beidler, D. R., Tewari, M., Friesen, P. D., Poirier, G. & Dixit, V. M. (1995). *J. Biol. Chem.* **270**, 16526–16528.

Bertin, J., Mendrysa, S. M., LaCount, D. J., Gaur, S., Krebs, J. F., Armstrong, R. C., Tomaselli, K. J. & Friesen, P. D. (1996). *J. Virol.* **70**, 6251–6259.
Bump, N. J., Hackett, M., Hugunin, M., Seshagiri, S., Brady, K., Chen, P., Ferenz, C., Ferenz, S., Franklin, S., Ghayur, T., Li, P., Licari, P., Mankovich, J., Shi, L., Greenberg, A. H., Miller, L. K. & Wong, W. W. (1995). *Science*, **269**, 1885–1888.
Cartier, J. L., Hershberger, P. A. & Friesen, P. D. (1994). *J. Virol.* **68**, 7728–7737.
Casciola-Rosen, L., Nicholson, D. W., Chong, T., Rowan, K. R., Thornberry, N. A., Miller, D. K. & Rosen, A. (1996). *J. Exp. Med.* **183**, 1957–1964.
Cohen, G. M. (1997). *Biochem. J.* **326**, 1–16.
delaCruz, W. P., Friesen, P. D. & Fisher, A. J. (2001). *J. Biol. Chem.* **276**, 32933–32939.
Fisher, A. J., delaCruz, W., Zoog, S. J., Schneider, C. L. & Friesen, P. D. (1999). *EMBO J.* **18**, 2031–2039.
Hardwick, J. M. (1997). *Adv. Pharmacol.* **41**, 295–336.
Hawkins, C. J., Yoo, S. J., Peterson, E. P., Wang, S. L., Vernooy, S. Y. & Hay, B. A. (2000). *J. Biol. Chem.* **275**, 27084–27093.
Kissinger, C. R., Gehlhaar, D. K. & Fogel, D. B. (1999). *Acta Cryst.* D**55**, 484–491.
Manji, G. A. & Friesen, P. D. (2001). *J. Biol. Chem.* **276**, 16704–16710.
Matthews, B. W. (1968). *J. Mol. Biol.* **33**, 491–497.
Nicholson, D. W. & Thornberry, N. A. (1997). *Trends Biol. Sci.* **22**, 299–306.
Otwinowski, Z. & Minor, W. (1997). *Methods Enzymol.* **276**, 307–326.
Rotonda, J., Nicholson, D. W., Fazil, K. M., Gallant, M., Gareau, Y., Labelle, M., Peterson, E. P., Rasper, D. M., Ruel, R., Vaillancourt, J. P., Thornberry, N. A. & Becker, J. W. (1996). *Nature Struct. Biol.* **3**, 619–625.
Shen, Y. & Shenk, T. E. (1995). *Curr. Opin. Genet. Dev.* **5**, 105–111.
Sugimoto, A., Friesen, P. D. & Rothman, J. H. (1994). *EMBO J.* **13**, 2023–2028.
Thompson, C. B. (1995). *Science*, **267**, 1456–1462.
Thornberry, N. A. & Lazebnik, Y. (1998). *Science*, **281**, 1312–1316.
Vier, J., Fürmann, C. & Häcker, G. (2000). *Biochem. Biophys. Res. Commun.* **276**, 855–861.
White, E. (1996). *Gen. Dev.* **10**, 1–15.
Xu, G. Z., Cirilli, M., Huang, Y. H., Rich, R. L., Myszka, D. G. & Wu, H. (2001). *Nature (London)*, **410**, 494–497.
Zhou, Q., Krebs, J. F., Snipas, S. J., Price, A., Alnemri, E. S., Tomaselli, K. J. & Salvesen, G. S. (1998). *Biochemistry*, **37**, 10757–10765.